doi:10.1093/brain/awn301 Brain 2009: 132; 250–259 | 250

BRAIN
A JOURNAL OF NEUROLOGY

Genotype–Phenotype correlations in multiple sclerosis: *HLA* genes influence disease severity inferred by ^{1}HMR spectroscopy and MRI measures

D. T. Okuda,[1] R. Srinivasan,[2] J. R. Oksenberg,[1] D. S. Goodin,[1] S. E. Baranzini,[1] A. Beheshtian,[1] E. Waubant,[1] S. S. Zamvil,[1] D. Leppert,[3] P. Qualley,[1] R. Lincoln,[1] R. Gomez,[1] S. Caillier,[1] M. George,[1] J. Wang,[1] S. J. Nelson,[2] B. A. C. Cree,[1] S. L. Hauser[1] and D. Pelletier[1]

1 Departments of Neurology, Multiple Sclerosis Center at UCSF, USA
2 Department of Radiology, University of California, San Francisco, California, USA
3 Neurologische Klinik, Universitätsspital Basel, Switzerland

Correspondence to: Daniel Pelletier, MD,
University of California, San Francisco,
UCSF Multiple Sclerosis Center,
350 Parnassus Avenue, Suite 908,
San Francisco, California 94117, USA
E-mail: daniel.pelletier@ucsf.edu

Genetic susceptibility to multiple sclerosis (MS) is associated with the human leukocyte antigen (HLA) *DRB1*1501* allele. Here we show a clear association between *DRB1*1501* carrier status and four domains of disease severity in an investigation of genotype–phenotype associations in 505 robust, clinically well characterized MS patients evaluated cross-sectionally: (i) a reduction in the *N*-acetyl-aspartate (NAA) concentration within normal appearing white matter (NAWM) via ^{1}HMR spectroscopy ($P = 0.025$), (ii) an increase in the volume of white matter (WM) lesions utilizing conventional anatomical MRI techniques (1,127 mm^3; $P = 0.031$), (iii) a reduction in normalized brain parenchymal volume (nBPV) ($P = 0.023$), and (iv) impairments in cognitive function as measured by the Paced Auditory Serial Addition Test (PASAT-3) performance (Mean *Z* Score: *DRB1*1501+*: 0.110 versus *DRB1*1501-*: 0.048; $P = 0.004$). In addition, *DRB1*1501+* patients had significantly more women (74% versus 63%; $P = 0.009$) and a younger mean age at disease onset (32.4 years versus 34.3 years; $P = 0.025$). Our findings suggest that *DRB1*1501* increases disease severity in MS by facilitating the development of more T2-foci, thereby increasing the potential for irreversible axonal compromise and subsequent neuronal degeneration, as suggested by the reduction of NAA concentrations in NAWM, ultimately leading to a decline in brain volume. These structural aberrations may explain the significant differences in cognitive performance observed between *DRB1*1501* groups. The overall goal of a deep phenotypic approach to MS is to develop an array of meaningful biomarkers to monitor the course of the disease, predict future disease behaviour, determine when treatment is necessary, and perhaps to more effectively recommend an available therapeutic intervention.

Keywords: multiple sclerosis; HLA; spectroscopy; brain atrophy; cognition

Abbreviations: HLA = human leukocyte antigen; MS = multiple sclerosis; NAA = *N*-acetyl-aspartate; NAWM = normal appearing white matter; nBPV = normalized brain parenchymal volume; PASAT = paced auditory serial addition test; WM = white matter

Received June 30, 2008. Revised September 25, 2008. Accepted October 20, 2008. Advance Access publication November 20, 2008

Introduction

The human leukocyte antigen (HLA) *DRB1∗1501-DQB1-0602* haplotype is a well-established risk factor for multiple sclerosis (MS) (Bertrams and Kuwert, 1972; Govaerts *et al*., 1985; Barcellos *et al*., 2003; Oksenberg *et al*., 2004; Hafler *et al*., 2007). Fine mapping data suggests that the *DRB1* gene itself is responsible for a significant portion of this risk (Ebers *et al*., 1996; Oksenberg *et al*., 2004). In Northern European populations, more than half of individuals with MS are *DRB1∗1501* positive, and even higher frequencies are observed in some familial MS cohorts (Haines *et al*., 1998; Rubio *et al*., 2002; Barcellos *et al*., 2006). Although *DRB1∗1501* is the best studied susceptibility allele in MS, the influence of the HLA region is complex (Haines *et al*., 1998; Barcellos *et al*., 2002; Sawcer *et al*., 2005; Yeo *et al*., 2007), and other *DRB1* variants can also contribute to MS risk, including *DRB1∗04* in Sardinians and Sicilians, and *DRB1∗1503* and *DRB1∗03* in African-Americans (Marrosu *et al*., 2002; Oksenberg *et al*., 2004; Brassat *et al*., 2005). *DRB1∗1501* also influences MS susceptibility in a dose-dependent fashion; homozygotes are at a several fold higher risk compared with heterozygotes (Barcellos *et al*., 2003). Although *DRB1* alleles clearly influence MS susceptibility, little is known about whether HLA variation influences clinical manifestations or outcomes in MS (Kantarci *et al*., 2002; Villoslada *et al*., 2002).

The current study was stimulated by our previous analysis of the Optic Neuritis Treatment Trial (ONTT) group, in which we reported that individuals carrying the *DRB1∗1501* allele exhibited higher numbers of focal brain lesions at the time of initial presentation with optic neuritis (Hauser *et al*., 2000). This observation suggested that *DRB1* genes might influence the radiological characteristics of MS patients at an early time point in their disease course. In the present study, we utilized a large, clinically well-characterized group of MS patients to further explore the relationship between neuroimaging parameters and *DRB1∗1501* carrier status. In addition to conventional anatomic MR end-points, we utilized an advanced proton spectroscopic metabolic imaging metric as a marker of neuronal integrity in regions of normal appearing white matter (NAWM), which have been reported to be significantly abnormal in MS compared to normal controls (Fu *et al*., 1998; Oh *et al*., 2004; Srinivasan *et al*., 2005), along with a fully automated, validated technique utilized in the assessment of normalized brain volume (Smith *et al*., 2001, 2007). The results of this analysis led us to test the hypothesis that there may be a clinical correlation with regard to cognitive performance and the radiological differences observed between patients who carry *DRB1∗1501* versus those that do not. Thus, we also report an association between the *HLA-DRB1∗1501* gene and cognitive function.

Methods

Research participants

The population was ascertained through a prospective study of phenotype–genotype-biomarker associations in a large cohort of MS patients followed longitudinally. Patients (aged 18–65 years) evaluated at the Multiple Sclerosis Center at the University of California, San Francisco (UCSF) between July 2004 and September 2005 were invited to participate. Patients with a recent onset of MS were preferentially recruited, although individuals with all clinical subtypes of the disease participated. These disease types included: clinically isolated syndrome (CIS), relapsing remitting MS (RRMS), secondary progressive MS (SPMS), primary progressive MS (PPMS), and progressive relapsing MS (PRMS). Patients were not entered if they had experienced a clinical relapse or received treatment with glucocorticosteroids within the previous month. The concomitant use of disease modifying therapies for MS was permitted. The protocol was approved by the Committee on Human Research at UCSF, and informed consent was obtained from all participants.

HLA-DRB1∗1501 typing

HLA-DRB1 genotypes were determined using a validated allele-specific TaqMan probe-based, 5′ nuclease assay specific for *DRB1∗1501*. High quality genomic DNA for all samples, including positive and negative controls, were organized, and 2 μl were aliquoted into 384 well plates for PCR amplification. An internal positive control (β-globin) was included in each well to confirm successful amplification of the reaction. PCR was carried out in a total volume of 10 μl, containing 20 ng DNA, 1 × TaqMan Universal PCR Master Mix (Applied Biosystems, Foster City, California), 0.6 μM *DRB1∗1501* specific primers, 0.3 μM control primers, 0.225 μM VIC-labeled *DRB1∗1501* probe, and 0.025 μM 6FAM-labeled control probe. Amplification was carried out in an ABI PRISM 7900HT Sequence Detection System (Applied Biosystems) with an initial 95°C cycle for 10 min, followed by 50 cycles of 95°C for 15 s and 62°C for 1 min. Samples were considered to contain at least one copy of the *DRB1∗1501* allele if the respective cycle exceeded a pre-established threshold.

Image acquisition

Brain MRI scans were performed on all subjects upon entry into the study, and analyses were carried out without knowledge of disease subtype, duration or treatment history. MRI images were acquired using an 8-channel phased array coil in reception and a body coil in transmission on a 3T GE Excite scanner (GE Healthcare Technologies, Waukesha, WI). Each MR imaging examination included scout localizers and axial dual-echo spin echo sequences (TE at 20 and 90 ms, TR = 2000 ms, 512 × 512 × 44 matrix, 240 × 240 × 132 mm^3 FOV, slice thickness = 3 mm, interleaved). A high-resolution inversion recovery spoiled gradient-echo T1-weighted isotropic, volumetric sequence (3D IRSPGR, 1 × 1 × 1 mm^3, 180 slices) was also performed (TE/TR/TI = 2/7/400 ms, flip angle = 15°, 256 × 256 × 180 matrix, 240 × 240 × 180 mm^3 FOV, NEX = 1). Conventional spin echo, T1-weighted images were acquired 5 min following administration of a single dose (0.1 mM/kg) of contrast agent (TE/TR = 8/467 ms, 256 × 256 × 44 matrix, 240 × 240 × 132 FOV, NEX = 1).

Brain lesions were identified by medical doctors (M.D.) specializing in MS (DTO, AB) on simultaneously viewed high-resolution T1-weighted, T2-weighted, and proton density-weighted images. Regions of interest (ROI) were drawn based on a semi-automated threshold with manual editing utilizing in-house software, and T1-lesion masks created; the process described elsewhere (Blum *et al*., 2002). Both intra and inter-observer variability analyses were performed to ensure the accuracy of data acquired. T2-lesion volumes from ROI selections were calculated by multiplying the area of the lesion by the slice thickness and the number of slices penetrated

using in-house software. A qualitative analysis for the presence of gadolinium enhancement was performed on post-contrast T1-weighted images.

Brain tissue segmentation and normalization

Brain segmentation and normalization was performed using SIENAX (Image Analysis Group, Oxford, UK), a fully automated technique. T1-lesion masks (described above) were presented to the SIENAX programme to correct for misclassifications of parenchymal tissue while T1-weighted images were segmented into images representing the volume of each voxel containing grey matter (GM), WM, cerebral spinal fluid (CSF), and WM lesion. The lesion masks overrode all SIENAX tissue classifications. Normalized tissue volumes were calculated by summing the lesion corrected, partial volume estimate maps, multiplied by the brain scalling factor calculated by the SIENAX programme yielding the normalized brain parenchymal volume (nBPV).

Spectral acquisition and quantification

TE-Averaged MRSI spectra were acquired with an in-plane resolution of 1.2×1.0 cm over a single slice of thickness 1.5 cm in the supratentorial brain just above the corpus callosum (Srinivasan *et al*., 2006). The spectroscopic data were acquired on a 3T GE Excite scanner (GE Healthcare Technologies, Waukesha, WI) using an 8-channel phased coil immediately following the acquisition of the anatomical images and prior to the administration of the contrast agent. The resulting coil combination data were TE-averaged and the metabolic concentration of N-acetyl-aspartate (NAA) were obtained using an LCmodel quantification algorithm and corrected for T1 and T2 relaxation times using similar methods described elsewhere (Ratiney *et al*., 2007). Only metabolite estimates within 5% Cramer-Rao error estimates were included in the analysis.

Parameter estimates in 'Pure' grey and white matter

Non-brain regions were removed from the anatomical images using a semi-automated brain extraction tool. T1-weighted images were segmented into GM, WM, and CSF compartments using a hidden Markov random field model with expectation maximization (Zhang *et al*., 2001). The GM and WM maps were re-grid to the spectroscopic resolution and convolved with the point spread function for spectroscopic imaging to yield the percent GM and WM content within each spectroscopic voxel. By modelling the NAA concentrations and MR relaxation parameters as a linear function of WM content, 'pure' GM and WM NAA concentrations were extrapolated from the endpoints of the linear fit (Hetherington *et al*., 1996; Noworolski *et al*., 1999).

Clinical measures

For all subjects, the Expanded Disability Status Scale (EDSS) (Kurtzke *et al*., 1983), Multiple Sclerosis Functional Composite (MSFC) (Fischer *et al*., 1999), Functional Assessment in MS (FAMS), and brain MR scans (described above) were performed within 2 weeks of entry into the study. CIS was defined as the first well-defined neurological event lasting $\geqslant$48 h, involving the optic nerve, spinal cord, brainstem, or cerebellum. In CIS patients, the presence of two or more hyperintense lesions on a T2-weighted MRI sequence was also required for enrollment into the study. The diagnosis of RRMS was made utilizing the new International Panel criteria (McDonald *et al*., 2001; Polman *et al*., 2005). SPMS was defined by 6 months of worsening neurological disability not explained by clinical relapse; deterioration was measured as either: (i) an increase of one or more points on the EDSS in patients with scores $<$6.0, or (ii) an increase of one-half point or more for those with EDSS scores $\geqslant$6.0. PPMS was defined both by (1) progressive clinical worsening for $>$12 months from symptom onset without any relapses, and (2) abnormal cerebrospinal fluid (CSF) as defined by the presence of $\geqslant$2 oligoclonal bands or an elevated IgG index. If acute relapses were superimposed on this steadily progressive course, patients were considered to have PRMS.

MS functional composite protocol

Three formally trained research coordinators at the UCSF MS Center administered the MSFC. Formal didactic descriptions and a standardized protocol for administering the MSFC were utilized for all patients. All examiners were blinded to MS subtype, *DRB1*1501* status, and radiological outcomes. Instructions were provided in English only. Testing order included: (i) 9-Hole Peg Test (9-HPT) (two timed trials of the dominant hand performed in succession followed by the assessment of the non-dominant hand), (ii) Paced Auditory Serial Addition Test (PASAT-3) (single trial with 3-s interstimulus intervals) and (iii) 25-Foot Timed Walk (25-FTW) (two-timed trials). Attempts were made to ensure that the same MSFC examiner performed all studies longitudinally for a given patient.

A single version of the PASAT (PASAT-3A), with score range from 0 to 60, was used. Directions were formally read to the patient and one to three practice runs of 11 pre-selected numbers with 10 possible responses provided prior to scoring. The test was aborted if patients were unable to provide at least two non-consecutive correct answers during the practice session. The test was also aborted, and number of correct responses determined, if a request was made during the evaluation for the test to be terminated.

MSFC scores were derived by the methods previously described by the National MS Society's Clinical Assessment Task Force (Fischer *et al*., 1999). Standardized scores (*Z*-scores) were calculated for the 9-HPT, PASAT-3, and 25-FTW representing the number of standard deviation units of performance from the reference population (entire MS cohort) mean. *Z*-Scores for the 9-HPT were calculated by averaging the two trial times for each hand followed by conversion to an averaged reciprocal time. The reciprocal mean performance time for the reference population was subtracted from the individual patient's averaged reciprocal time then divided by the reference population standard deviation. *Z*-scores for the 25-FTW were calculated by subtracting the average time from the reference population from the average of the two-timed 25-FTW trials then divided by the reference population standard deviation. PASAT-3 performance was calculated by determining the number of correct responses during a single trial using a 3-s stimulus interval. *Z*-scores were calculated by determining the difference between the patient's performance and reference population mean then divided by the reference population standard deviation.

The MSFC score was derived by the following equation:

$$\text{MSFC Score} = [(Z\text{-score 1/9-HPT}) + (-Z\text{-score 25-FTW}) + (Z\text{-score PASAT-3})]/3$$

Positive *Z*-scores represent the number of standard deviation units of performance better than the reference population mean.

FAMS

Self-Reported Questionnaires [FAMS (Version 4)] focusing on: (i) emotional well-being; (ii) thinking and fatigue, and (iii) pain were administered at baseline. Patients were advised to provide assessments based on their experience over the past 7 days. Scores ranging from 0 (not at all) to 4 (very much) were assigned to the emotional well-being (seven questions) and thinking and fatigue (nine questions) sections. A Pain Intensity Numerical Rating Scale ranging from 0 (no pain) to 10 (worst possible pain) was used to assess pain intensity associated with MS or MS treatments over the previous 12 months.

Statistical analysis

The frequency of *DRB1∗1501* was compared against gender, disease subtype, age of disease onset, disease duration, presence or absence of treatment, EDSS, T2-lesion volumes and gadolinium enhancement. Box–Cox transformation was performed on T2-lesion volumes prior to analysis for the treatment of non-normality (Box and Cox, 1964). Kolmogorov-Smirnov test for normality was performed on the transformed T2-lesion volumes and NAA concentrations. Analysis of Covariance (ANCOVA) was used to assess for differences in the transformed T2-lesion volumes between *DRB1∗1501* haplotypes. The differences between the adjusted mean values [least-squares means (LSMeans)] of the transformed T2-lesion volumes and NAA concentrations between haplotypes were compared using a Student's *T*-test. Multi-colinearity among the variables in the model was examined by assessing the tolerance. Linear regression analysis was used to study the association between *DRB1∗1501* carriers and NAA concentrations, Box–Cox transformed T2-lesion volumes, and nBPV measurements with relevant confounding variables incorporated in the model.

For the non-parametric analysis, the untransformed T2-lesion volumes were divided into quartiles from Q1 to Q4; with Q1 representing lowest lesion volumes and Q4 containing the highest lesion load. Logistic regression was used to assess the likelihood of *DRB1∗1501* patients falling into the higher quartiles compared to non-carriers. Data from Q1 was used as the reference category for calculating the odds ratios (ORs) and degree of significance (*P*-values). Potential confounding variables were included in the model.

A Wilcoxon Two-sample test was performed comparing baseline EDSS and FAMS scores in addition to 9-HPT, PASAT-3, and 25-FTW *Z*-scores along with overall MSFC performance between *DRB1∗1501+* and *DRB1∗1501-* MS patients. A generalized linear model (SAS v.9.1.3 GENMOD Procedure) was utilized, incorporating the maximum likelihood estimation for regression coefficients for important covariates in the model (age, age of disease onset, disease duration, prior exposure to immunotherapy, T2-lesion volumes, and baseline PASAT *Z*-scores) and likelihood ratio test to examine the *DRB1∗1501* effect. Multi-colinearity among the variables in the model was examined by assessing tolerance.

All statistical analyses were performed using SAS v.9.1.3 (SAS Institute Inc., North Carolina, USA). A *P*-value $\leqslant 0.05$ was considered statistically significant.

Results

A total of 511 patients were enrolled during the study period. Six patients were excluded due to motion artifact on the MRI scan ($n=2$) or lack of the appropriate MR dual-echo sequence performed for lesion volume determination ($n=4$). Of the 505 cases available, the specific MS subtypes included: 88 CIS, 352 RRMS, 46 SPMS, 14 PPMS, three PRMS, and two patients with an uncertain MS subtype. Table 1 summarizes the clinical data for the entire cohort. The distribution of the clinical and demographic data divided on the basis of *DRB1∗1501* haplotypes (either positive or negative) is shown in Table 2. The *DRB1∗1501+* group had significantly more women (74% versus 63%; $P=0.009$) and a younger mean age at disease onset (32.4 years versus 34.3 years; $P=0.025$) compared to the *DRB1∗1501-* group.

Spectroscopic metabolic data were acquired from 409 patients (1501+: 185, 1501-: 224) of the 505 cases available (81%). Table 3 summarizes the demographic and clinical data for these patients. A significantly lower concentration of NAA in the NAWM was observed in the *DRB1∗1501+* group ($P=0.025$), with similar mean concentrations of NAA identified in NAGM ($P=0.221$). Linear regression analysis incorporating significant covariates (e.g. gender, age of disease onset, T2-lesion volume, and disease duration) on the effect of NAA concentration in NAWM continued to demonstrate a statistically significant concentration reduction in the *DRB1∗1501+* group ($P<0.05$).

Using ANCOVA, a greater value of the transformed and adjusted T2-lesion volume, consistent with a higher burden of disease, was found for the *DRB1∗1501+* group (see Methods for details of this analysis). Back transformation of the adjusted

Table 1 Summary of the demographic and clinical data for the entire study cohort

	N		Mean	Median	Range
Age (Y)	503		42.1	42.0	17–65
Gender	505	F: 344(68%); M: 161(32%)			
Age of disease onset (Y)	503		33.5	33.0	11–60
Disease duration (Y)	503		9.68	7.00	1.0–46.0
MS treatment exposure	505	YES: 348(69%); NO: 157(31%)			
HLA-DRB1*1501	505	1501+: 232(46%); 1501-: 273(54%)			
EDSS score	505		2.0	1.5	0.0–7.0
N-Acetyl-Aspartate – NAWM (mM)	409		9.96	9.89	6.86–14.47
MSFC score	487		0.051	0.208	−4.920–1.186
T2-Lesion load (mm^3)	503		7365.2	3082.3	0.0–87641.0
Normalized brain parenchymal volume (cm^3)	504		1588.8	1600.9	1270.0–1821.9

Y = years; F = female; M = male; EDSS = expanded disability status scale; NAWM = normal appearing white matter; MSFC = multiple sclerosis functional composite.

Table 2 Summary of demographic and clinical data by *HLA-DRB1*1501* haplotype

	*HLA-DRB1*1501*		Mean	SD	Median	*P*-value
Age (Y)	1501+		41.4	9.9	41	0.116
	1501−		42.7	9.8	43	
Gender	1501+	F: 171(74%); M: 60 (26%)				**0.009**
	1501−	F: 173(63%); M: 101(37%)				
Age of disease onset (Y)	1501+		32.4	8.8	32	**0.025**
	1501−		34.3	9.7	34	
Disease duration (Y)	1501+		9.99	8.5	7.0	0.170
	1501−		9.41	9.2	6.0	
MS treatment exposure	1501+	YES: 163(71%); NO: 68(29%)				0.462
	1501−	YES: 185(68%); NO: 89(32%)				
HLA-DRB1*1501	1501+	232 (46%)				0.609
	1501−	273 (54%)				
EDSS score	1501+		1.9	1.6	1.5	0.201
	1501−		2.1	1.7	2.0	
MSFC score	1501+		0.082	0.631	0.197	0.434
	1501−		0.034	0.710	0.223	
9-Hole peg test[a]	1501+		0.003	0.958	0.116	0.738
	1501−		0.017	1.027	0.097	
PASAT-3[a]	1501+		0.110	1.070	−0.128	**0.004**
	1501−		0.048	0.935	0.266	
25-FTW[a]	1501+		0.017	0.789	−0.0001	0.119
	1501−		0.120	1.149	0.0329	
T2-Lesion load (mm^3)	1501+		8109.8	13006	3337.1	**0.031**
	1501−		6786.2	10137	2828.5	
Normalized brain parenchymal volume (cm^3)	1501+		1585.9	90.3	1589.6	**0.023**
	1501−		1591.4	88.6	1607.6	
Volume scaling factor	1501+		1.33	0.11	1.33	0.600
	1501−		1.34	0.12	1.33	

a *Z* Score. Y = years; F = female; M = male; EDSS = expanded disability status scale; MSFC = multiple sclerosis functional composite; PASAT = paced auditory serial addition test; 25-FTW = 25-Foot timed walk.

Table 3 Summary of the demographic and clinical data for patients undergoing ^{1}HMR analysis

	N		Mean	SD	Median	Range
Age (Y)	409		43.9	9.8	43.5	18.0–66.9
Gender	409	F: 274(67%); M: 135(33%)				
Age of disease onset (Y)	409		33.6	9.4	33.0	11.0–59.0
Disease duration (Y)	409		10.0	9.0	7.1	0.0–46.0
MS treatment exposure	409	YES: 282(69%); NO: 127(31%)				
HLA-DRB1*1501	409	1501+: 185(45%); 1501−: 224(55%)				
EDSS score	409		2.3	1.7	2.0	0.0–7.0
N-Acetyl-Aspartate – NAWM (mM)	409		9.96	1.28	9.89	6.86–14.47
1501+ ($N = 185$) $P = 0.025$			9.80	1.30	9.70	6.86–14.47
1501− ($N = 224$)			10.10	1.30	10.10	7.12–13.67
T2-Lesion load (mm^3)	409		7211.2	10972.9	3151.5	0.0–86610.3

Y = years; F = female; M = male; EDSS = expanded disability status scale; NAWM = normal appearing white matter.

Table 4 Summary of the demographic and clinical data by T2-lesion load quartiles

	Q1	Q2	Q3	Q4
T2-Lesion load (mm^3)	*N* = 126 Mean = 335.07 SD = 254.38 Median = 297.62 Range: 0–887.92	*N* = 126 Mean = 1889.45 SD = 631.06 Median = 1882.95 Range: 915.60–3082.32	*N* = 126 Mean = 5336.18 SD = 1527.66 Median = 5121.50 Range: 3119.24–8738.09	*N* = 125 Mean = 22016.27 SD = 15222.37 Median = 16386.55 Range: 8864.65–87641.24
Age (Y) *P* = 0.030	*N* = 125 Mean = 39.9 SD = 9.1 Median = 40.0 Range: 17–65	*N* = 125 Mean = 41.9 SD = 9.6 Median = 42.0 Range: 18–64	*N* = 126 Mean = 42.8 SD = 9.7 Median = 41.5 Range: 23–63	*N* = 125 Mean = 43.7 SD = 10.8 Median = 43.0 Range: 19–65
Gender *P* = 0.652	F: 87 (25.5%) M: 39 (24.1%)	F: 87 (25.5%) M: 39 (24.0%)	F: 88 (25.8%) M: 38 (23.5%)	F: 79 (23.2%) M: 46 (28.4%)
Age at disease onset (Y) *P* < 0.0001	*N* = 125 Mean = 34.5 SD = 8.6 Median = 35.0 Range: 13–55	*N* = 125 Mean = 35.2 SD = 8.6 Median = 35.0 Range: 17–58	*N* = 126 Mean = 33.6 SD = 9.7 Median = 32.0 Range: 17–60	*N* = 125 Mean = 30.3 SD = 9.4 Median = 29.7 Range: 11–58
Disease duration (Y) *P* < 0.0001	*N* = 125 Mean = 6.5 SD = 6.5 Median = 4.0 Range: 1–35	*N* = 125 Mean = 7.7 SD = 7.1 Median = 5.0 Range: 1–38	*N* = 126 Mean = 10.2 SD = 8.6 Median = 7.0 Range: 1–37	*N* = 125 Mean = 14.4 SD = 10.7 Median = 12.0 Range: 1–46
MS treatment exposure *P* < 0.0001	NO: 59 (47.2%) YES: 66 (52.8%)	NO: 36 (28.8%) YES: 89 (71.2%)	NO: 34 (27.0%) YES: 92 (73.0%)	NO: 27 (21.6%) YES: 98 (78.4%)
HLA-DRB1*1501 *P* = 0.066	1501+: 45 (19.7%) 1501−: 80 (29.4%)	1501+: 64 (28.0%) 1501−: 61 (22.4%)	1501+: 62 (27.2%) 1501−: 62 (22.8%)	1501+: 57 (25.0%) 1501−: 69 (25.4%)
EDSS score *P* < 0.0001	*N* = 125 Mean = 1.58 SD = 1.50 Median = 1.5 Range: 0–7	*N* = 125 Mean = 1.77 SD = 1.46 Median = 1.5 Range: 0–6	*N* = 126 Mean = 1.97 SD = 1.43 Median = 1.5 Range: 0–6	*N* = 125 Mean = 2.72 SD = 1.93 Median = 2.0 Range: 0–7

Y = years; F = female; M = male; EDSS = expanded disability status scale.

means showed a 1,127 mm^3 greater lesion volume in the *DRB1∗1501* group compared to all other *DRB1* alleles (*P* = 0.031).

Non-parametric statistical methods were used to compare the quartiles for untransformed T2-lesion volumes and to confirm the results obtained from the parametric statistical analysis. Gender (*P* = 0.652) and *HLA-DRB1∗1501* status (*P* = 0.066) were not associated with T2-lesion volume (Table 4). By contrast, age (*P* = 0.030), age at disease onset (*P* < 0.0001), disease duration (*P* < 0.0001), previous exposure to immunotherapy (*P* < 0.0001) and EDSS (*P* < 0.0001) were associated with greater T2-lesion volumes. *DRB1∗1501*+ subjects classified with CIS, RRMS, and SPMS were 1.90 times (*P* = 0.015) more likely to have higher T2-lesion volumes with values falling into Q2 versus Q1 and 1.69 times more likely to fall into Q3 versus Q1 (*P* = 0.049) when age of disease onset, duration of disease, and *DRB1∗1501* status were included as predictors. Significant differences were not observed in the ORs when comparing Q4 versus Q1 (*P* = 0.314). Logistic regression did not reveal substantial differences in the ORs or statistical significance with the addition of potentially confounding covariates (Table 5). Inclusion of the PPMS and PRMS subtypes revealed similar ORs and degrees of significance between quartiles (data not shown).

Linear regression analysis, incorporating significant covariates (i.e. age of disease onset, gender, duration of disease, EDSS, and exposure to treatment), revealed a significant reduction in nBPV for the *DRB1∗1501*+ group with a least squares mean difference of 14 cm^3 (*P* = 0.023) observed, representing a 0.9% reduction in the total brain volume between *DRB1∗1501* carriers and non-carriers. No significant difference was observed in the normalized scalling factors for both groups.

Analysis of the impact of *DRB1∗1501* on cognitive function revealed a statistically significant difference in PASAT-3 performance between haplotypic groups (*P* = 0.004), a result that remained significant after a sensitivity analysis for potential confounders (*P* < 0.005). Patient age, disease duration, EDSS, FAMS, and MSFC scores, along with exposure to immunotherapy, the type of such therapy, and the presence of gadolinium enhancing lesions were similar between groups.

Table 5 Logistic regression analysis and effect of potential confounders on T2-lesion load volume

	Logistic regression equation	R^2	Q2/Q1 Odds ratio 95% CI	Q3/Q1 Odds ratio 95% CI	Q4/Q1 Odds ratio 95% CI
RR/SP/CIS ($N = 483$)	T2LL = AODO + DD + *DRB1*1501*	0.15	1.90 **$P = 0.015$** 1.13–3.20	1.69 **$P = 0.049$** 1.00–2.86	1.32 $P = 0.314$ 0.77–2.29
RR/SP/CIS ($N = 483$)	T2LL = AODO + DD + EDSS + *DRB1*1501*	0.18	1.92 **$P = 0.014$** 1.14–3.23	1.74 **$P = 0.039$** 1.03–2.94	1.38 $P = 0.258$ 0.79–2.40
RR/SP/CIS ($N = 482$)	T2LL = AODO + TX + DD + *DRB1*1501*	0.19	1.97 **$P = 0.012$** 1.16–3.33	1.76 **$P = 0.038$** 1.03–3.00	1.39 $P = 0.245$ 0.80–2.43
RR/SP/CIS ($N = 482$)	T2LL = AODO + TX + DD + EDSS + *DRB1*1501*	0.21	1.97 **$P = 0.012$** 1.16–3.35	1.79 **$P = 0.032$** 1.05–3.06	1.44 $P = 0.210$ 0.82–2.52

RR = relapsing-remitting MS; SP = secondary-progressive MS; CIS = clinically isolated syndrome; T2LL = T2-lesion load; AODO = age of disease onset; DD = disease duration; TX = exposure to MS treatment.
Significance of bold values is $P \leqslant 0.05$.

Discussion

An effect of the *HLA-DRB1∗1501* gene on four domains of disease severity in MS was identified: (i) a reduction in NAA concentration within NAWM by MR spectroscopy suggesting alterations in neuronal integrity not discernable through conventional techniques, (ii) a higher adjusted mean T2-lesion volume utilizing conventional MR measures, (iii) reduced normalized brain volume utilizing high-resolution images, and (iv) impairments in cognitive function as measured by PASAT-3 performance. Taken together, these data, derived from a large and prospectively ascertained population, indicate that *DRB1∗1501* increases disease severity in MS by facilitating the development of more T2-foci, which has the potential of transecting axons, leading to widespread axonal compromise (reduction of NAA in NAWM) and subsequent degeneration with resultant brain atrophy and associated injury suggested by the presence of cognitive impairment (decline in PASAT-3 performance).

Disease-modifying therapies for MS, used by many patients in the cohort, were unlikely to have influenced the outcomes reported here. The proportion of patients treated with interferon (IFN), glatiramer acetate (GA), or immune suppression was similar between the *DRB1∗1501+* and *DRB1∗1501-* groups, as was the total duration of treatment. One earlier unconfirmed study with limited power suggested the presence of an interaction between *DRB1∗1501* and a treatment response to GA (Fusco *et al*., 2001). However, this effect, if present, would have biased results in the opposite direction to those observed here (i.e. GA treated *DRB1∗1501+* patients would have been expected to accumulate fewer focal MS lesions). We previously reported, in a different population of MS patients, that responses to IFN are not influenced by DR status (Villoslada *et al*., 2002). Interestingly, the influence of *DRB1∗1501* on T2-lesion volume appeared to decrease as the total burden of disease increased. With increasing T2-lesion volume there is less remaining normal WM at risk for demyelination, which could slow the accumulation of new focal lesions and blunt any inter-group differences.

The metabolite N-acetyl-aspartic acid is principally viewed as a marker of neural integrity, because of its high concentration in neurons, dendrites, axons, and synapses in the CNS (Birken and Oldendorf, 1989; Simmons *et al*., 1991). NAA concentrations are known to be reduced in chronic MS lesions (van Walderveen *et al*., 1999), a finding interpreted as neuronal or axonal loss, although questions remain unanswered with regard to the dynamic nature of NAA changes and their reversibility or irreversibility (Oh *et al*., 2004). Previous studies of NAA in NAWM employed single-voxel MRS techniques that have lower spatial resolution than the 2D multi-voxel modality used in this study, precluding firm associations from being identified. In an earlier study of NAWM in the corpus callosum of MS patients, we reported reduced NAA values (Oh *et al*., 2004). In RRMS and SPMS, these MR outcomes were strongly influenced by the presence of distant pericallosal MS lesions, consistent with a secondary degenerative process (i.e. Wallerian degeneration) occurring in normal appearing brain regions. The difference observed here in NAA concentrations suggest that a reduction in axonal density or integrity is associated with the presence of *DRB1∗1501*. Longitudinal studies are in progress, and these should better define the evolution of spectroscopic metabolite concentrations in normal appearing brain regions, especially as patients transition from the relapsing to the progressive stage of MS.

Cognitive impairment in MS is a common cause of clinical disability in MS, and a symptom that exhibits discordant features with the degree of motor impairment (Piras *et al*., 2003). That *DRB1∗1501* patients have a higher T2 burden of disease and reduced brain parenchymal volume suggested the possibility of a difference in cognitive impairment in *DRB1∗1501* patients compared to other *DRB1* alleles. T2-lesion volume and brain atrophy

were previously correlated with the evolution of cognitive decline in MS (Rao *et al*., 1989, 1991; Piras *et al*., 2003; Houtchens *et al*., 2007). The presence of T2-foci is directly associated with irreversible axonal transection and compromise (Trapp *et al*., 1998); thereby providing an explanation for previous studies demonstrating the association between burden of disease and cognitive integrity. Compromises in cognitive function, signified by PASAT-3 performance, may also be related to subsequent secondary degeneration, as observed in our dataset with significant changes noted between *DRB1∗1501* groups and brain volumes normalized for intracranial skull size. Investigations correlating both semi and fully automated whole brain volumetric techniques to cognitive performance in MS are nascent and definitive data controlling for important covariates are deficient. More recently, NAA concentration and executive function in healthy individuals were also correlated, suggesting alterations in brain integrity not appreciated with conventional techniques (Charlton *et al*., 2007). Efforts were made in this study to ensure that fatigue and mood disorders were not potential contributors to a decline in PASAT-3 performance. The lack of statistical differences in self-reported FAMS scores suggests that these were not significant contributing factors. It is likely that the correlations between NAA, T2-lesion volume, nBPV and PASAT-3 observed here provide overlapping evidence for an association between *HLA-DRB1∗1501* and MS severity (Fig. 1).

The gene products of *DRB1∗1501* in white populations, and the closely related *DRB1∗1503* in blacks, share in common a structurally related hydrophobic peptide-binding motif facilitating tight binding to aromatic amino acids that includes the critical aa92 (Phe) residue of the 89–96 region of myelin basic protein (MBP). This peptide sequence is known to be immunodominant in *DRB1∗1501* individuals, resulting in efficient presentation of MBP 89–96, or a related cross-reactive (possibly viral) peptide, to T cells (Ota *et al*., 1990; Wucherpfennig *et al*., 1994, 1995), specific activation of T cells in the circulation of *DRB1∗1501* individuals with MS (Allegretta *et al*., 1990; Scholz *et al*., 1998), and the presence of 89–96 MBP reactive T cells in MS plaques (Oksenberg *et al*., 1993). By analogy to animal models of T cell mediated autoimmune demyelination (Zamvil *et al*., 1985), early in the disease course focal lesions may result from a relatively limited number of pathogenic T cell specificities. Over time, epitope spreading may occur, increasing the number of autoantigen targets recognized by pathogenic T cells and the diversity of HLA restricting elements mediating the disease. We would speculate that, in *DRB1∗1501*+ individuals with MS, high numbers of MBP-reactive T cells stochastically favour the development of more focal lesions early in the disease course, and also greater concentration of encephalitogenic T cells in lesions favouring secondary axonal degeneration measured as loss of NAA in NAWM. Continued intra- and inter-molecular epitope spreading, as well as the development of pathogenic T cell responses not restricted to *DRB1∗1501*, could modulate this effect of *DRB1∗1501* over time. This biologically plausible mechanism, in addition to the lack of neurodegeneration observed without inflammation in animal models (Lorentzen *et al*., 1995; Zhou *et al*., 2006), supports our rationale of a mechanistic cascade of disease severity.

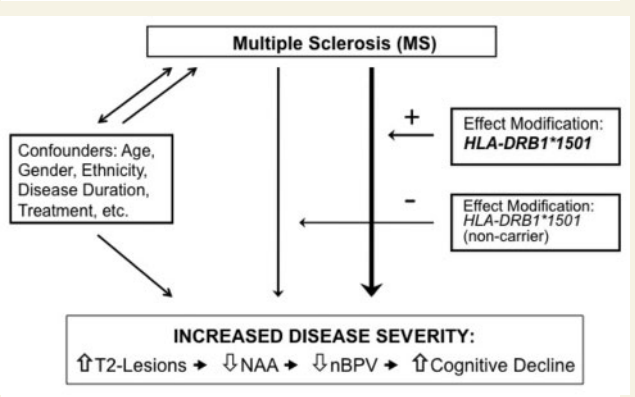

Fig. 1 Schematic representation of the relationship between MS and disease severity with the influence of confounders, in addition to the effect modifier, *HLA-DRB1∗1501*, that is proposed to facilitate increased brain injury. A unidirectional arrow indicates a causal association. A non-causal relationship is indicated by the bidirectional arrow.

In summary, these results demonstrate a robust association between the *DRB1∗1501* haplotype and MS disease severity. An association between *DRB1∗1501* and disease severity, as measured by spectroscopic metabolic differences, with a reduction in the concentration of NAA in NAWM was observed; the result of an increased burden of disease observed on conventional anatomic imaging as well as disease in NAWM not yet discernable utilizing conventional MRI techniques. These imaging findings, along with alterations in nBPV between groups, are likely responsible for the alterations in cognitive integrity observed. Longitudinal studies—combining imaging, genetic, and clinical variables, in addition to other biomarkers are currently underway to test and extend these cross-sectional findings. These technologies offer a remarkable opportunity to investigate heterogeneity in MS. In another example, we have recently reported that expression profiling of CD4 cells can robustly predict the future behaviour of CIS patients for period of 1 year (Corvol *et al*., 2008). The overall goal of a deep phenotypic approach to MS is to develop an array of meaningful biomarkers to monitor the course of the disease, predict its future behaviour, determine when treatment is necessary, and perhaps also select from among available therapies. Longitudinal studies, combining imaging, genetic, and clinical outcomes, in addition to other biomarkers, are currently underway to affirm and extend these novel data. Similar studies and results from independent datasets would also provide additional confirmation. Overall, these efforts are likely to substantially clarify the underlying biology of MS.

Acknowledgements

We are grateful to our patients who generously agreed to serve as study participants. We thank W. Chin, H. Mousavi, and R. Guerrero for sample preparation and repository management. Dr Daniel Pelletier is a Harry Weaver Neuroscience Scholar of the U.S. National Multiple Sclerosis Society (JF#2122).

Funding

National Institutes of Health (NS26799, AI067152, R01 NS049477, U19 AI067152); National Multiple Sclerosis Society (RG#3517); and a research grant from GlaxoSmithKline; and gifts from the Signe Ostby Foundation and the Friends of Amy.

References

Allegretta M, Nicklas JA, Sriram S, Albertini RJ. T cells responsive to myelin basic protein in patients with multiple sclerosis. Science 1990; 247: 718–21.

Barcellos LF, Oksenberg JR, Green AJ, Bucher P, Rimmler JB, Schmidt S, et al. Genetic basis for clinical expression in multiple sclerosis. Brain 2002; 125: 150–8.

Barcellos LF, Oksenberg JR, Begovich AB, Martin ER, Schmidt S, Vittinghoff E, et al. HLA-DR2 dose effect on susceptibility to multiple sclerosis and influence on disease course. Am J Hum Genet 2003; 72: 710–6.

Barcellos LF, Sawcer S, Ramsay PP, Baranzini SE, Thomson G, Briggs F, et al. Heterogeneity at the HLA-DRB1 locus and risk for multiple sclerosis. Hum Mol Genet 2006; 15: 2813–24.

Bertrams J, Kuwert E. HL-A antigen frequencies in multiple sclerosis. Significant increase of HL-A3, HL-A10 and W5, and decrease of HL-A12. Eur Neurol 1972; 7: 74–8.

Birken DL, Oldendorf WH. N-acetyl-L-aspartic acid: a literature review of a compound prominent in 1H-NMR spectroscopic studies of brain. Neurosci Biobehav Rev 1989; 13: 23–31.

Blum D, Yonelinas AP, Luks T, Newitt D, Oh J, Lu Y, et al. Dissociating perceptual and conceptual implicit memory in multiple sclerosis patients. Brain Cogn 2002; 50: 51–61.

Box GEP, Cox DR. An analysis of transformations. J Roy Stat Soc 1964; B-26: 211–52.

Brassat D, Salemi G, Barcellos LF, McNeill G, Proia P, Hauser SL, et al. The HLA locus and multiple sclerosis in Sicily. Neurology 2005; 64: 361–3.

Charlton RA, McIntyre DJ, Howe FA, Morris RG, Markus HS. The relationship between white matter brain metabolites and cognition in normal aging: the GENIE study. Brain Res 2007; 1164: 108–16.

Corvol J-C, Pelletier D, Henry R, Caillier SJ, Wang J, Pappas D, et al. Abrogation of T cell quiescence characterizes patients at high risk for multiple sclerosis after the initial neurological event. Proc Natl Acad Sci USA 2008; 105: 11839–44.

Ebers GC, Kukay K, Bulman DE, Sadovnick AD, Rice G, Anderson C, et al. A full genome search in multiple sclerosis. Nat Genet 1996; 13: 472–6.

Fischer JS, Rudick RA, Cutter GR, Reingold SC. The multiple sclerosis functional composite measure (MSFC): an integrated approach to MS clinical outcome assessment. National MS society clinical outcomes assessment task force. Mult Scler 1999; 5: 244–50.

Fusco C, Andreone V, Coppola G, Luongo V, Guerini F, Pace E, et al. HLA-DRB1*1501 and response to copolymer-1 therapy in relapsing-remitting multiple sclerosis. Neurology 2001; 57: 1976–79.

Fu L, Matthews PM, De Stefano N, Worsley KJ, Narayanan S, Francis GS, et al. Imaging axonal damage of normal-appearing white matter in multiple sclerosis. Brain 1998; 121: 103–13.

Govaerts A, Gony J, Martin-Mondiere C, Poirier JC, Schmid M, Schuller E, et al. HLA and multiple sclerosis: population and families study. Tissue Antigens 1985; 25: 187–99.

Hafler DA, Compston A, Sawcer S, Lander ES, Daly MJ, De Jager PL, et al. Risk alleles for multiple sclerosis identified by a genomewide study. N Engl J Med 2007; 357: 851–62.

Haines JL, Terwedow HA, Burgess K, Pericak-Vance MA, Rimmler JB, Martin ER, et al. Linkage of the MHC to familial multiple sclerosis suggests genetic heterogeneity. The multiple sclerosis genetics group. Hum Mol Genet 1998; 7: 1229–34.

Hauser SL, Oksenberg JR, Lincoln R, Garovoy J, Beck RW, Cole SR, et al. Interaction between HLA-DR2 and abnormal brain MRI in optic neuritis and early MS. Optic neuritis study group. Neurology 2000; 54: 1859–61.

Hetherington HP, Pan JW, Mason GF, Adams D, Vaughn MJ, Twieg DB, et al. Quantitative 1H spectroscopic imaging of human brain at 4.1 T using image segmentation. Magn Reson Med 1996; 36: 21–9.

Houtchens MK, Benedict RH, Killiany R, Sharma J, Jaisani Z, Singh B, et al. Thalamic atrophy and cognition in multiple sclerosis. Neurology 2007; 69: 1213–23.

Kantarci OH, de Andrade M, Weinshenker BG. Identifying disease modifying genes in multiple sclerosis. J Neuroimmunol 2002; 123: 144–59.

Kurtzke JF. Rating neurologic impairment in multiple sclerosis: an expanded disability status scale (EDSS). Neurology 1983; 33: 1444–52.

Lorentzen JC, Issazadeh S, Storch M, Mustafa MI, Lassman H, Linington C, et al. Protracted, relapsing and demyelinating experimental autoimmune encephalomyelitis in DA rats immunized with syngeneic spinal cord and incomplete Freund. J Neuroimmunol 1995; 63: 193–205.

Marrosu MG, Lai M, Cocco E, Loi V, Spinicci G, Pischedda MP, et al. Genetic factors and the founder effect explain familial MS in Sardinia. Neurology 2002; 58: 283–8.

McDonald WI, Compston A, Edan G, Goodkin D, Hartung HP, Lublin FD, et al. Recommended diagnostic criteria for multiple sclerosis: guidelines from the International Panel on the diagnosis of multiple sclerosis. Ann Neurol 2001; 50: 121–7.

Noworolski SM, Nelson SJ, Henry RG, Day MR, Wald LL, Star-Lack J, et al. High spatial resolution 1H-MRSI and segmented MRI of cortical gray matter and subcortical white matter in three regions of the human brain. Magn Reson Med 1999; 41: 21–9.

Oh J, Henry RG, Genain C, Nelson SJ, Pelletier D. Mechanisms of normal appearing corpus callosum injury related to pericallosal T1 lesions in multiple sclerosis using directional diffusion tensor and 1H MRS imaging. J Neurol Neurosurg Psychiatry 2004; 75: 1281–6.

Oksenberg JR, Barcellos LF, Cree BA, Baranzini SE, Bugawan TL, Khan O, et al. Mapping multiple sclerosis susceptibility to the HLA-DR locus in African Americans. Am J Hum Genet 2004; 74: 160–7.

Oksenberg JR, Begovich AB, Erlich HA, Steinman L. Genetic factors in multiple sclerosis. JAMA 1993; 270: 2362–9.

Ota K, Matsui M, Milford EL, Mackin GA, Weiner HL, Hafler DA. T-cell recognition of an immunodominant myelin basic protein epitope in multiple sclerosis. Nature 1990; 346: 183–7.

Piras MR, Magnano I, Canu ED, Paulus KS, Satta WM, Soddu A, et al. Longitudinal study of cognitive dysfunction in multiple sclerosis: neuropsychological, neuroradiological, and neurophysiological findings. J Neurol Neurosurg Psychiatry 2003; 74: 878–85.

Polman CH, Reingold SC, Edan G, Filippi M, Hartung HP, Kappos L, et al. Diagnostic criteria for multiple sclerosis: 2005 revisions to the 'McDonald Criteria'. Ann Neurol 2005; 58: 840–6.

Rao SM, Leo GJ, Haughton VM, St Aubin-Faubert P, Bernardin L. Correlation of magnetic resonance imaging with neuropsychological testing in multiple sclerosis. Neurology 1989; 39: 161–6.

Rao SM, Leo GJ, Bernardin L, Unverzagt F. Cognitive dysfunction in multiple sclerosis. I. Frequency, patterns, and prediction. Neurology 1991; 41: 685–91.

Ratiney H, Noworolski SM, Sdika M, Srinivasan R, Henry RG, Nelson SJ, et al. Estimation of metabolite T1 relaxation times using tissue specific analysis, signal averaging and bootstrapping from magnetic resonance spectroscopic imaging data. Magma 2007; 20: 143–55.

Rubio JP, Bahlo M, Butzkueven H, van Der Mei IA, Sale MM, Dickinson JL, et al. Genetic dissection of the human leukocyte antigen region by use of haplotypes of Tasmanians with multiple sclerosis. Am J Hum Genet 2002; 70: 1125–37.

Sawcer S, Ban M, Maranian M, Yeo TW, Compston A, Kirby A, et al. A high-density screen for linkage in multiple sclerosis. Am J Hum Genet 2005; 77: 454–67.

Scholz C, Patton KT, Anderson DE, Freeman GJ, Hafler DA. Expansion of autoreactive T cells in multiple sclerosis is independent of exogenous B7 costimulation. J Immunol 1998; 160: 1532–8.

Simmons ML, Frondoza CG, Coyle JT. Immunocytochemical localization of N-acetyl-aspartate with monoclonal antibodies. Neuroscience 1991; 45: 37–45.

Smith SM, De Stefano N, Jenkinson M, Matthews PM. Normalized accurate measurement of longitudinal brain change. J Comp Assist Tomography 2001; 3: 466–75.

Smith SM, Rao A, De Stefano N, Jenkinson M, Schott JM, Matthews PM, et al. Longitudinal and cross-sectional analysis of atrophy in Alzheimer's disease: cross-validation of BSI, SIENA and SIENAX. Neuroimage 2007; 36: 1200–6.

Srinivasan R, Cunningham C, Chen A, Vigneron D, Hurd R, Nelson S, et al. TE-averaged two-dimensional proton spectroscopic imaging of glutamate at 3 T. Neuroimage 2006; 30: 1171–8.

Srinivasan R, Sailasuta N, Hurd R, Nelson S, Pelletier D. Evidence of elevated glutamate in multiple sclerosis using magnetic resonance spectroscopy at 3 T. Brain 2005; 128: 1016–25.

Trapp BD, Peterson J, Ransohoff RM, Rudick R, Mork S, Bo L. Axonal transection in the lesions of multiple sclerosis. N Engl J Med 1998; 338: 278–85.

van Walderveen MA, Barkhof F, Pouwels PJ, van Schijndel RA, Polman CH, Castelijns JA. Neuronal damage in T1-hypointense multiple sclerosis lesions demonstrated in vivo using proton magnetic resonance spectroscopy. Ann Neurol 1999; 46: 79–87.

Villoslada P, Barcellos LF, Rio J, Begovich AB, Tintore M, Sastre-Garriga J, et al. The HLA locus and multiple sclerosis in Spain. Role in disease susceptibility, clinical course and response to interferon-beta. J Neuroimmunol 2002; 130: 194–201.

Wucherpfennig KW, Hafler DA. A review of T-cell receptors in multiple sclerosis: clonal expansion and persistence of human T-cells specific for an immunodominant myelin basic protein peptide. Ann N Y Acad Sci 1995; 756: 241–58.

Wucherpfennig KW, Zhang J, Witek C, Matsui M, Modabber Y, Ota K, et al. Clonal expansion and persistence of human T cells specific for an immunodominant myelin basic protein peptide. J Immunol 1994; 152: 5581–92.

Yeo TW, De Jager PL, Gregory SG, Barcellos LF, Walton A, Goris A, et al. A second major histocompatibility complex susceptibility locus for multiple sclerosis. Ann Neurol 2007; 61: 228–36.

Zamvil S, Nelson P, Trotter J, Mitchell D, Knobler R, Fritz R, et al. T-cell clones specific for myelin basic protein induce chronic relapsing paralysis and demyelination. Nature 1985; 317: 355–8.

Zhang Y, Brady M, Smith S. Segmentation of brain MR images through a hidden Markov random field model and the expectation-maximization algorithm. IEEE Trans Med Imaging 2001; 20: 45–57.

Zhou D, Srivastava R, Nessler S, Grummel V, Sommer N, Bruck W, et al. Identification of a pathogenic antibody response to native myelin oligodendrocyte glycoprotein in multiple sclerosis. Proc Natl Acad Sci USA 2006; 103: 19057–62.